Ambient Mechanosynthesis of Flexible Two-dimensional Covalent Organic Frameworks

Yogendra Nailwal,[a] Bryson Baker,[b] Ziad Alsudairy,[a,c] Mustapha El Hariri El Nokab,[d] Qingsong Zhang,[e] Tuo Wang,[d] Songliang Cai,[f] Yi Liu,[e] Xinle Li[a]*

[a] Department of Chemistry, Clark Atlanta University, Atlanta, Georgia 30314, United States

[b] Department of Chemistry, Howard University, Washington, DC 20059, USA

[c] Department of Chemistry, College of Science, Qassim University, Buraidah 51452, Saudi Arabia

[d] Department of Chemistry, Michigan State University, East Lansing, Michigan 48824, United States

[e] The Molecular Foundry, Lawrence Berkeley National Laboratory, One Cyclotron Road, Berkeley, California 94720, United States

[f] School of Chemistry, Guangzhou Key Laboratory of Analytical Chemistry for Biomedicine, South China Normal University, Guangzhou 510006, P. R. China

Abstract

Flexible two-dimensional covalent organic frameworks (2D COFs) constructed from nonplanar building blocks are highly sought after due to their structural uniqueness. Nevertheless, the prevailing solvothermal synthesis suffers from low time efficiency, environmental unfriendliness, and cumbersome protocols. Here, we address these challenges by developing the first ambient mechanosynthesis of a diverse library of flexible 2D COFs. Sixteen distinct triazine-cored Schiff-base COFs, including five as-yet-unreported ones, were rapidly synthesized via ball milling using 2,4,6-tris(4-aminophenoxy)-1,3,5-triazine (TPT-NH_2) and 2,4,6-tris(4-formylphenoxy)-1,3,5-triazine (TPT-CHO) as building blocks. Notably, the representative COF, MC-flexible-COF-1, was synthesized in as little as one hour under mechanosynthesis conditions, whereas it remained unattainable via the traditional solvothermal method, despite prolonged heating and extensive solvent screening. The highly dynamic nature of imine linkage was unequivocally demonstrated through mechanosynthesis-enabled imine exchange in molecular model compounds. Furthermore, MC-flexible-COF-1 exhibited a high uptake capacity of ~4.2 g g^{-1} in the adsorption of aqueous iodine pollutants. This work underscores the immense potential of mechanochemistry as a powerful and sustainable tool for the rapid synthesis of advanced 2D COFs, including those inaccessible via conventional solution-based methods.

Introduction

Two-dimensional covalent organic frameworks (2D COFs) are layered crystalline, porous, polymer networks interlinked by strong covalent bonds.[1] Their inherent structural attributes such as lightweight, high porosity, well-ordered skeletons, customizable functionalities, and superb stability, make them highly appealing for a wide array of applications, including gas separation,[2] heterogeneous catalysis,[3] drug delivery,[4] energy storage,[5] sensing,[6] environmental remediation,[7] proton conduction,[8] among others. 2D COFs are typically constructed from rigid, planar organic building blocks, which restrict rotational freedom and thus minimize the occurrence

of structural defects, such as extended faults and packing errors during crystallization. [9] While the use of rigid monomers is essential for achieving the high crystallinity of 2D COFs, it also limits their structural diversity and flexibility. To this end, developing novel COFs from flexible building blocks has garnered substantial attention in recent years. Extensive research efforts have been devoted to synthesizing COFs using flexible building units, particularly those based on 2,4,6-triaryloxy-1,3,5-triazine,[10] such as 2,4,6-tris(4-formylphenoxy)-1,3,5-triazine (TPT-CHO) and 2,4,6-tris(4-aminophenoxy)-1,3,5-triazine (TPT-NH_2). The emergent class of flexible triazine-cored 2D COFs exhibit unique physicochemical properties, which have demonstrated significant potential for diverse applications.[11] For instance, Chen and co-workers synthesized two flexible 2D COFs using TPT-CHO as the building block, and the resulting COFs displayed high adsorption capacity for both Rhodamine B and volatile iodine.[12] Zhang and co-workers subsequently reported a luminescent flexible 2D COF derived from TPT-CHO, showing highly sensitive and selective detection of picric acid.[13] Most recently in 2024, Pandey and co-workers developed four flexible triazine-cored 2D COFs, which exhibited exceptional performance in supercapacitor and CO_2 capture. Despite the substantial strides, the synthesis of flexible 2D COFs predominantly relies on solvothermal methods, which suffer from key drawbacks including long reaction times (typically 3 days), high energy consumption, adverse environment effects due to the use of toxic solvents, meticulous reaction setup associated with the deoxygenation process, and limited scalability.[14] These synthetic barriers significantly impeded the broad application and structural diversification of flexible COFs. Consequently, there is an urgent need to develop a generic synthetic route to obtain flexible COFs under milder conditions.

The past decade has witnessed a surge of scientific interest in exploring ambient and expeditious synthesis methods for COFs.[15] Notable strategies include: (i) exploring innovative energy sources such as mechanical agitation, ultrasound, electron beam, and gamma-ray irradiation.[16] (ii) developing new catalysts such as metal triflates, nitrates, or organic Lewis acid;[17] and (iii) employing aqueous conditions or alcohol/water mixtures.[18] Among these strategies, mechanochemistry, a transformative synthetic methodology that harnesses mechanical force to drive chemical transformations, offers notable advantages,[19] including (i) environmental benignity due to minimal solvent usage; (ii) rapid reaction times, ranging from minutes to hours; (iii) operational simplicity by circumventing tedious protocols such as freeze-pump-thaw and flame sealing; (iv) enhanced scalability owing to its solid-state nature; and (v) access products that are otherwise challenging to obtain through conventional solution-based methods. While the mechanosynthesis of organic molecules, polymers, inorganic nanomaterials, and metal-organic frameworks (MOFs) has been extensively studied for decades,[20] the exploration of mechanochemistry in COFs is still in its nascent stage. The first mechanosynthesis of COFs dates back to 2013 when the Benerjee group synthesized three *β*-ketoenamine-linked 2D COFs using a mortar and pestle.[21] Thereafter, the same group developed the liquid-assisted grinding method (2014) and salt-meditated crystallization approach (2017) in COF mechanochemistry.[22] In recent years, COF mechanochemistry has garnered escalating scientific interest, leading to the rapid and sustainable synthesis of various 2D COFs with linkages like Schiff base,[22-23] triazine,[24] and boroxine,[25] as well as COF composites with metal ions,[26] enzyme,[27] polyoxometalates,[28] and silica.[29] Despite remarkable progress in greener and faster synthesis of COFs, the full potential of

mechanochemistry is impeded by two key factors: the predominant reliance on rigid, planar monomers for 2D COF synthesis and the limited attempts of creating COFs inaccessible via solution-based methods. To address this gap, we propose that mechanochemistry offers a simple, rapid, and environmentally benign route for synthesizing flexible 2D COFs, including those hard to obtain in solution. To the best of our knowledge, the ambient mechanosynthesis of flexible 2D COFs remains hitherto uncharted.

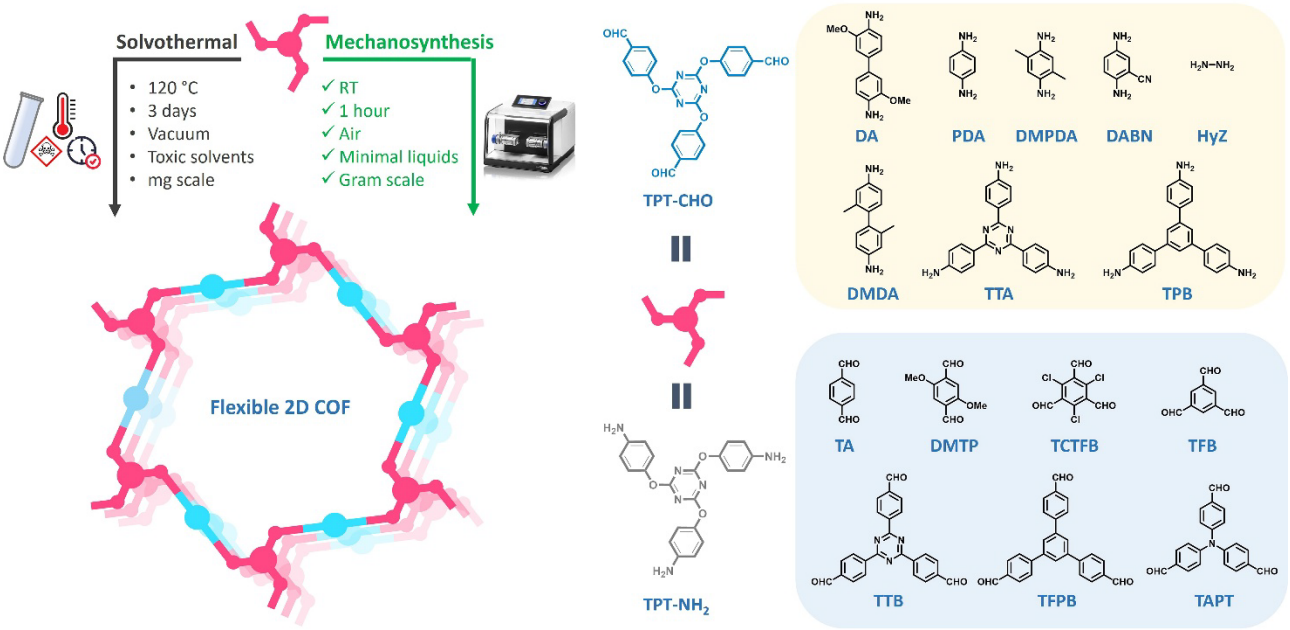

Scheme 1. Schematic representation of ambient, rapid, liquid-assisted mechanosynthesis of flexible triazine-based 2D COFs, in contrast to traditional solvothermal routes.

In this study, we showcase the first ambient, rapid, liquid-assisted mechanosynthesis of flexible Schiff-base 2D COFs using triazine-based trialdehyde and triamine as primary building blocks. In total, 16 different COFs bearing varied pore sizes, pendant functionalities, Schiff-base linkages, and core structures, including 5 previously unreported COFs, were prepared in only one hour at room temperature with minimal solvent usage. This method can be easily scaled to the half-gram scale without compromising COF quality. One representative COF was systematically investigated to elucidate the influence of mechanosynthesis parameters. Most notably, this approach enabled the efficient synthesis of a COF inaccessible by traditional solution-phase methods. To shed light on the mechanochemical COF formation, imine exchange reactions of model compounds were utilized to probe the dynamic nature of imine bonds under mechanical force. Furthermore, this mechanochemically synthesized COF exhibited a high adsorption capability of 4.3 ± 0.2 g g^{-1} toward aqueous I_3^-.

Results and Discussion

Initially, a flexible imine-linked 2D COF (denoted as MC-flexible-COF-1, MC represents mechanochemistry), derived from 2,4,6-tris(4-formylphenoxy)-1,3,5-triazine (TPT-CHO) and

3,3'-dimethoxy-[1,1'-biphenyl]-4,4'-diamine (BD-OMe), was selected as a benchmark system to optimize mechanosynthesis parameters (Figure 1a). Ambient mechanosynthesis of MC-flexible-COF-1 was conducted by ball-milling TPT-CHO and BDOMe in a 5 mL stainless steel jar containing one 5 mm stainless steel ball under aerobic conditions. To optimize the crystallinity of COF, several synthetic parameters were fine-tuned, including liquid additives, catalyst concentration, milling frequency, and reaction time (Figure 1). The COF quality was assessed using powder X-ray diffraction (PXRD) analysis. We commenced by optimizing liquid additives for mechanosynthesis. A mixture of mesitylene and acetonitrile (ACN) was found to be optimal when compared to mesitylene, ACN, and mesitylene/dioxane (Figure 1b and Table S1). Next, the influence of acetic acid (AcOH) catalyst concentration on COF formation was examined. Increasing the AcOH concentration up to 17.4 M AcOH progressively enhanced the COF's crystallinity (Figure 1c). Similarly, milling frequency plays an essential role in the mechanosynthesis of flexible 2D COF. Systematic variation of the milling frequency from 5 Hz to 30 Hz revealed an optimum at 20 Hz (Figure 1d). A too-high milling frequency hampered the COF crystallinity, consistent with our previous work on imine COF mechanosynthesis.[23a] To gain a better understanding of the COF formation, a rigorous ex-situ kinetic study was conducted. Gratifyingly, MC-flexible-COF-1 exhibited a prominent (100) Bragg diffraction peak at $2\theta = 2.2^{o}$ after a mere 1 minute of ball-milling under ambient conditions. The intensity of the characteristic reflections increased progressively at 5, 10, and 30 minutes, reaching the maximum at 1 h (Figure 1e). Ultimately, the optimal condition for ambient mechanosynthesis of MC-flexible-COF-1 was established: mesitylene/ACN as liquid additives ($\eta = 0.88$ μL mg^{-1}), glacial AcOH as the catalyst, a milling frequency of 20 Hz, and a milling time of 1 h. Under this condition, powdered MC-flexible-COF-1 was obtained with a dark yellow color in a high yield of 76% (Figure S1).

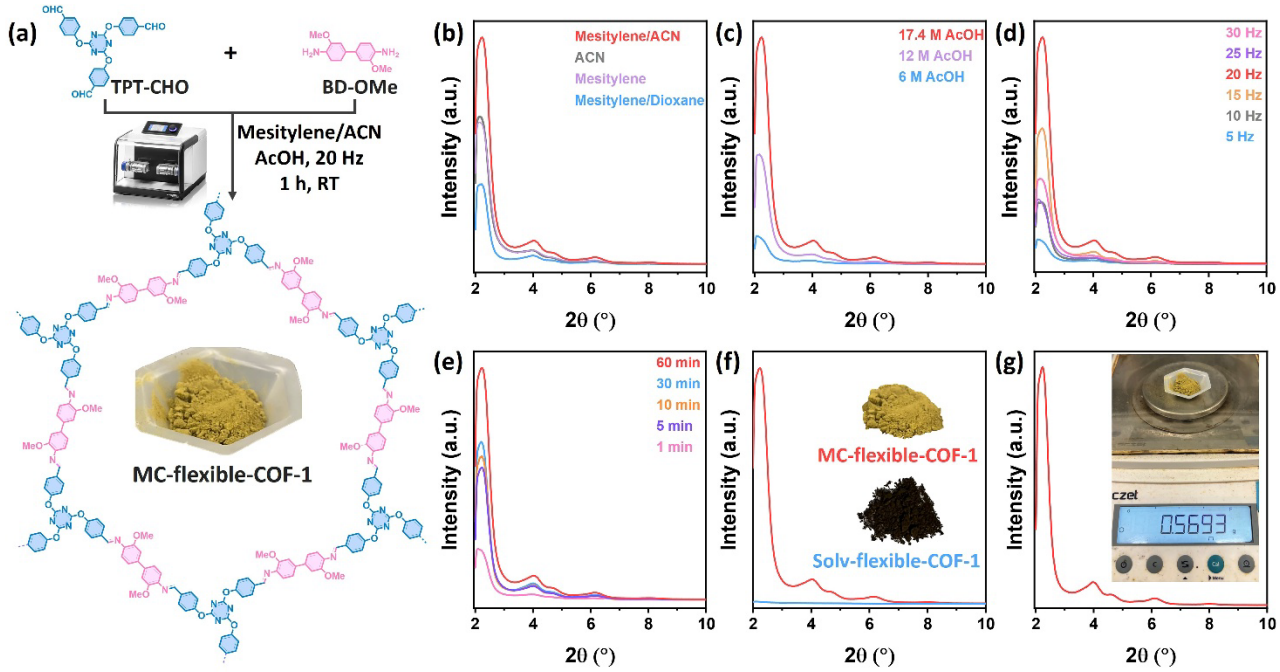

Figure 1. Ambient mechanosynthesis of MC-flexible-COF-1. (a) Schematic of MC-flexible-COF-1 via ball-milling synthesis at ambient conditions. PXRD patterns of MC-flexible-COF-1 with variation of (b) liquid additives, (c) catalyst concentration, (d) milling frequency, and (e) milling time. (e) PXRD patterns of MC-flexible-COF-1 and solv-flexible-POP-1, inset is their physical appearance; (f) Gram-synthesis of MC-flexible-COF-1.

To further highlight the advantages of mechanosynthesis, we opted for the preparation of the solvothermal analog of flexible-COF-1 using traditional solution methods. Despite extensive optimization of solvothermal conditions (Table S2), including variations in solvents, reaction times (up to 4 days), atmosphere, and temperatures (80-120 °C), we failed to obtain the crystalline product (Figure S2). In certain conditions, even no precipitates were formed (Table S2). In stark contrast, the mechanosynthesis enabled the effective synthesis of highly crystalline MC-flexible-COF-1 in as little as minutes. The PXRD pattern of MC-flexible-COF-1 displayed sharp and distinct diffraction peaks, conspicuously absent in the amorphous solv-flexible-POP-1 (Figure 1f). Furthermore, their visual differences were striking: MC-flexible-COF-1 exhibited a dark yellow color whereas solv-flexible-POP-1 appeared deep brown (inset image, Figure 1f), signifying partial oxidation during the solvothermal process. These marked contrasts in physical appearance, crystallinity, and synthetic outcomes underscore the unparalleled advantages of mechanosynthesis, as it not only provides an environmentally benign route to COFs but also enables the synthesis of COFs inaccessible via traditional solution-based methods.[19] In addition, the large-scale synthesis of COFs, a critical prerequisite for industrial applications, has long been a formidable challenge.[30] Given its exceptional scalability in chemical synthesis, mechanochemistry offers a promising solution. To assess the scalability of our mechanosynthesis, a gram-scale reaction was conducted using a 25 mL stainless steel jar, yielding 0.57 g of highly crystalline MC-flexible-COF-1 in just 1 h (Figure 1f). This result further underscores the practicality of mechanosynthesis for the large-scale production of high-quality flexible 2D COFs.

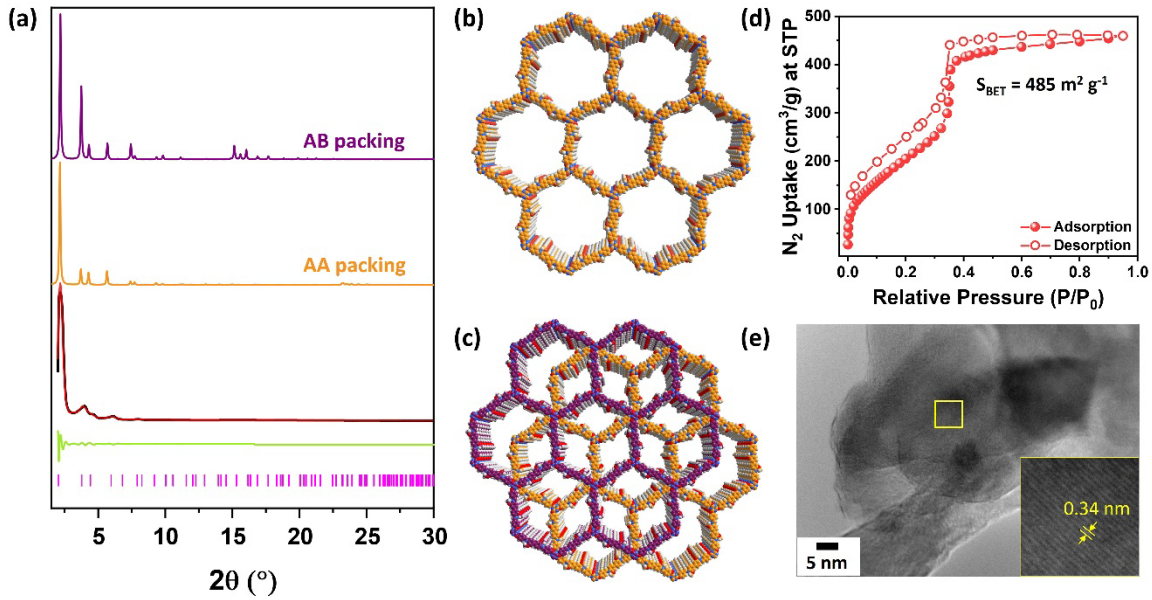

Figure 2. (a) PXRD profiles of MC-flexible-COF-1. Experimental (black), Pawley refined (red), and their difference (green), simulated pattern using the AA stacking mode (purple) and the staggered AB stacking mode (orange). (b) The unit cell of the AA stacking mode. (c) The unit cell of the AB stacking mode. (d) N_2 adsorption-desorption isotherm; (e) TEM images of MC-flexible-COF-1, inset; zoomed-in TEM image of the marked yellow area showing periodic lattice fringes.

The obtained MC-flexible-COF-1 was thoroughly characterized by a suite of analytical techniques. Fourier transform infrared (FTIR) spectrum of MC-flexible-COF-1 showed the disappearance of the characteristic-CHO stretch at 1693 cm^{-1} from TPT-CHO and -NH_2 stretch at 3429 cm^{-1} from BD-OMe, alongside the emergence of a new -C=N stretch at 1626 cm^{-1}, indicating the successful imine condensation (Figure S3). The presence of imine linkage was further corroborated by solid-state ^{13}C cross-polarization magic angle spinning (CP-MAS) NMR spectroscopy (Figure S4). The ^{13}C CP-MAS NMR spectrum of MC-flexible-COF-1 revealed a peak at 157 ppm, corresponding to imine carbons. In addition, the prominent peaks at 174 ppm and 55 ppm were attributed to the triazine carbons and methoxy carbons, respectively.

The crystalline structure of MC-flexible-COF-1 was confirmed by PXRD analysis and structural simulation. The PXRD pattern of MC-flexible-COF-1 revealed five prominent reflection peaks, with the most intense one at $2\theta = 2.22°$ (FWHM = 0.46°) and additional reflections at 2θ = 3.97, 4.57, 6.12, 8.02 and 26.82°, corresponding to the (100), (110), (200), (210), (220), and (001) facets, respectively (Figure 2a, red curve). To elucidate the unit cell parameters of MC-flexible-COF-1, eclipse AA and staggered AB stacking modes were modeled in space group *P*6 (Figure 2). The experimental PXRD pattern closely matched the pattern simulated from the AA stacking mode (Figure 2a, orange curve), whereas it deviated from the one from the AB stacking mode (Figure 2a, purple curve). Furthermore, Pawley refinement provided a good fit to the experimental PXRD pattern (Figure 2a, red curve), as evidenced by the minimal difference between the simulated and experimental profiles (Figure 2a, green curve). The Pawley refinement yielded a unit cell of $a = b$ = 44.63 Å, c = 3.48 Å, $\alpha = \beta = 90°$, $\gamma = 120°$ with good agreement factors (R_{WP} = 4.68%, R_P = 6.08%). The permanent porosity of MC-flexible-COF-1 was evaluated by N_2 uptake analysis. A Type IV sorption isotherm with a hysteresis loop suggested the mesoporous nature of the COF (Figure 2d). The Brunauer-Emmett-Teller (BET) surface area was calculated to be 485 $m^2 g^{-1}$ for MC-flexible-COF-1, higher than those obtained in 1-minute and 10-minute milling (Figures S5 and S6). The morphology of MC-flexible-COF-1 was investigated using scanning electron microscopy (SEM) and transmission electron microscopy (TEM). SEM images revealed the layered aggregates with relative sizes of 30−50 μm for MC-flexible-COF-1 (Figure S7). TEM imaging also confirmed the 2D layered sheet morphology and exhibited periodic lattice fringes with a *d*-spacing of 0.34 nm (Figure 2e, S8), corresponding to the (001) lattice plane of MC-flexible-COF-1. This value also aligns with the calculated interlayer distance of 0.33 nm from the (001) reflection in the PXRD pattern. Moreover, thermogravimetric analysis (TGA) indicated the high thermal stability of MC-flexible-COF-1 up to 350 °C under anaerobic (N_2) conditions (Figure S9).

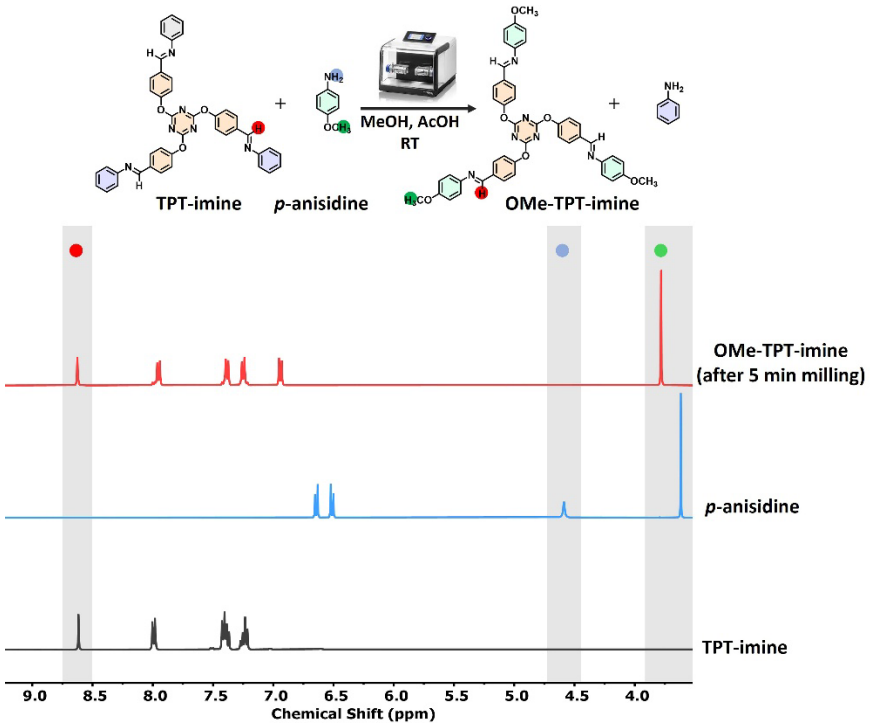

Figure 3. Mechanosynthesis-enabled imine exchange to probe the dynamic imine reactivity under mechanical force.

The reversible nature of covalent bonds governs the crystallinity of 2D COFs, as it enables the dynamic breaking and reformation of in-plane bonds within the COF lattice, ultimately driving the system toward its thermodynamic minimum.[31] We hypothesize that the reversibility of imine bonds under mechanosynthesis conditions plays a pivotal role in the rapid formation of flexible COFs. To probe the dynamic nature of imine bonds under ball milling conditions, we performed a "scrambling" experiment between a model triazine-cored imine analog (TPT-imine) with *p*-anisidine (Figure 3). The solid mixture was subjected to ball milling in the presence of catalytic acetic acid under ambient conditions and the resulting products were analyzed by solution-phase ^{1}H NMR spectroscopy. Remarkably, after only 5 minutes of ball-milling, ^{1}H NMR analysis revealed the emergence of a singlet at 3.8 ppm, characteristic of the methoxy group in the newly formed OMe-TPT-imine, confirming the rapid occurrence of the imine exchange reaction under nearly-solid-state conditions. This result provides compelling evidence for the highly dynamic nature of imine bonds under mechanochemical conditions, which is poised to be responsible for the rapid formation of highly crystalline flexible 2D COFs.

To showcase the generality of the mechanosynthesis strategy, we synthesized additional 15 flexible 2D COFs from various amine and aldehyde monomers (Figure 4). These [C_3 + C_2] and [C_3 + C_3] polymerizations were conducted for the construction of 2D COFs with different pore sizes, pendant groups, and Schiff-base linkages (i.e., imine, azine, and *β*-ketoenamine). Of these, 10 COFs have been previously reported and were predominantly prepared via conventional solution-based methods. It is worth noting that the mechanosynthesis strategy enabled the synthesis of these COFs with moderate-to-high crystallinity: TPT-CHO-DMDA (MC-flexible-

COF-2),[32] TPT-CHO-PDA (MC-flexible-COF-3),[11] TPT-CHO-TTA (MC-flexible-COF-6),[33] TPT-CHO-TPB (MC-flexible-COF-7),[34] TPT-CHO-TPT-NH_2 (MC-flexible-COF-9),[34] TPT-NH_2-TFB (MC-flexible-COF-10),[16b] TPT-NH_2-DMTP (MC-flexible-COF-11),[16b] TPT-NH_2-TTB (MC-flexible-COF-12),[16b] TPT-NH_2-TFPB (MC-flexible-COF-13),[16b] and TPT-NH_2-TA (MC-flexible-COF-14).[33] The PXRD profiles (Figures S10-S24) and FTIR spectra (Figures S25-S40) of the obtained COFs were in good agreement with previous data in the literature. Taken together, this mechanosynthesis method is broadly applicable, affording a wide range of flexible 2D COFs at ambient conditions within an hour.

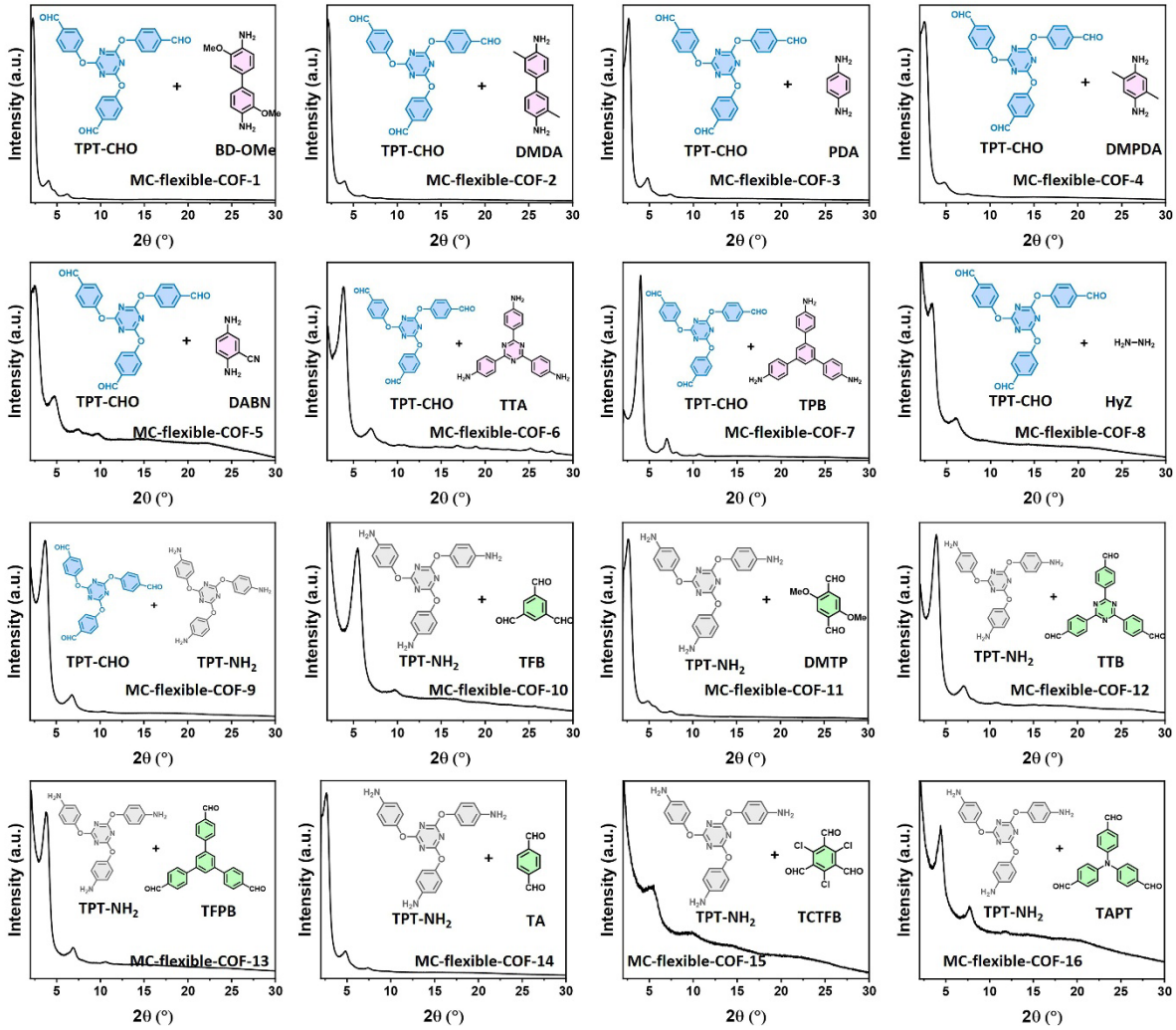

Figure 4. The broad applicability of mechanosynthesis of 2D MC-flexible-COFs under ambient conditions.

The excessive emission of iodine into groundwater from industrial sources poses a significant threat to both aquatic ecosystems and human health, necessitating the development of high-performance adsorbents for aqueous iodine removal.[35] Encouraged by the heteroatom-rich and ordered pore channels of MC-flexible-COFs, we investigated their potential as adsorbents for

capturing triiodide (I_3^-) from aqueous solutions. To evaluate this, MC-flexible-COF-1 was introduced into a 10 mL aqueous solution of I_2/KI (150 ppm I_2 and 250 ppm KI), where I_3^- forms via the equilibrium reaction $I_2 + I^- \rightleftharpoons I_3^-$. The adsorption process was monitored using UV-vis spectroscopy, tracking the characteristic absorption peaks of I_2 (290 nm) and I_3^- (350 nm) (Figure 5a). A kinetic study revealed that MC-flexible-COF-1 rapidly removed approximately 80% of iodine within 20 minutes (Figure 5b). The maximum I_3^- uptake capacity was evaluated by immersing MC-flexible-COF-1 in a concentrated I_2/KI (4 mM) aqueous solution for 3 days. The maximum iodine uptake capacity of MC-flexible-COF-1 was calculated to be 4.3 ± 0.2 g g^{-1} (Figure 5c), surpassing many previously reported COF adsorbents (Figure 5d, Table S18).[36] Adsorption kinetics of MC-flexible-COF-1 were best described by the pseudo-second-order model, exhibiting a high correlation coefficient (R^2) value of 0.999 (Figure S41). Furthermore, the selectivity of a I_3^- in the iodine solution by MC-flexible-COF-1 was examined in the presence of competing anions such as SO_4^{2-}, Cl^-, NO_3^-, CH_3COO^-, and CO_3^{2-}. Remarkably, MC-flexible-COF-1 demonstrated excellent selectivity towards I_3^- over these anions, revealing excellent binding affinity for I_3^- (Figure S42). The reusability of MC-flexible-COF-1 adsorbent was evaluated by cycling experiment. After each adsorption cycle, MC-flexible-COF-1 was washed with methanol and dried at 120 °C under a vacuum for use in the next cycle. After three cycles, the I_3^- adsorption capability of MC-flexible-COF-1 decreased to 90% of the initial value (Figure S43), accompanied by a loss of crystallinity in a I_3^--loaded MC-flexible-COF-1. Notably, the crystallinity was restored upon the removal of iodine from the COF (Figure S44).

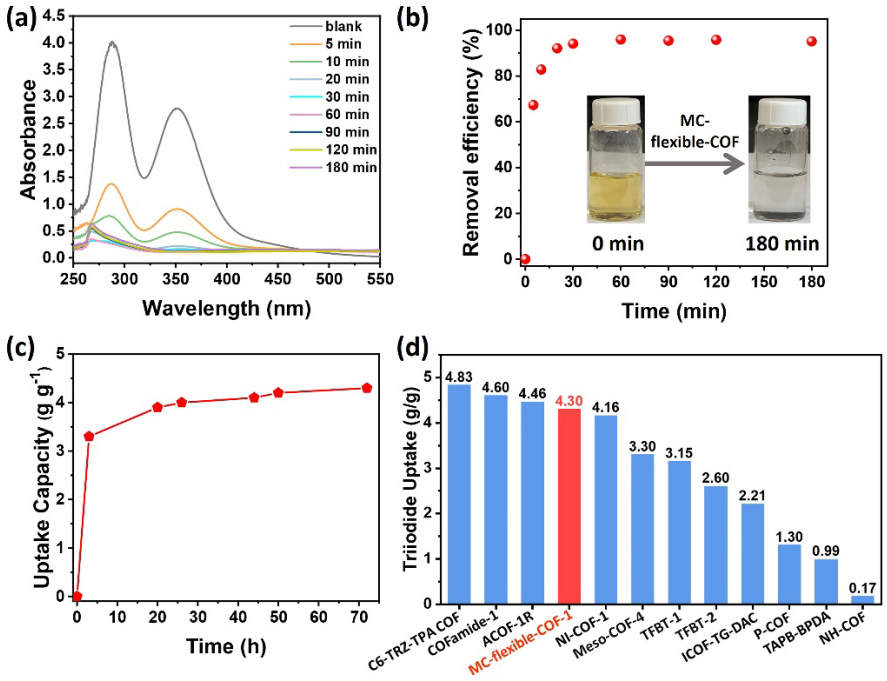

Figure 5. (a) UV-vis spectra of I_3^- adsorption by MC-flexible-COF-1 in I_2/KI aqueous solution. (b) Removal efficiency of I_3^- by MC-flexible-COF-1. (c) Maximum I_3^- adsorption isotherm of MC-flexible-COF-1in I_2/KI solution. (d) Aqueous triiodide (I_3^-) adsorption capacities of MC-flexible-COF-1 and previously reported COF sorbents.

Conclusion

In conclusion, we have developed the first mechanosynthesis of a diverse library of flexible 2D COFs from triazine-based monomers under ambient conditions. This rapid and nearly solventless method enabled the synthesis of 16 distinct Schiff-base COFs within one hour, offering significant advantages over traditional solvothermal methods in terms of efficiency, sustainability, simplicity, scalability, and versatility. Importantly, mechanochemistry enabled the efficient synthesis of MC-flexible-COF-1, which was unattainable through traditional solution-based methods. Mechanochemical imine exchange studies in molecular model compounds have revealed the highly dynamic nature of imine linkage under mechanical force, which plays an essential role in the rapid formation of flexible COFs. Furthermore, MC-flexible-COF-1 demonstrated a high adsorption capability of 4.3 ± 0.2 g g^{-1} for aqueous iodine pollutants, outperforming numerous previously reported COF adsorbents. This study unlocks the full potential of mechanochemistry for the sustainable and rapid synthesis of novel COFs, thereby expediting their discovery and enhancing their industrial prospects.

Conflicts of interest

There are no conflicts to declare.

Acknowledgements

This work is funded by the U.S. Department of Energy Early Career Award (DE-SC0022000), the National Science Foundation HBCU-UP-RIA program (no. 2100360), the PREC program (no. 2216807), and the PREM program (DMR-2122147). Part of the work was carried out at the Molecular Foundry as a user project, supported by the Office of Science, Office of Basic Energy Sciences, of the U.S. Department of Energy under Contract No. DE-AC02-05CH11231.

References

[1] C. S. Diercks, O. M. Yaghi, *Science* **2017**, *355*, eaal1585.
[2] C. Ma, X. Li, J. Zhang, Y. Liu, J. J. Urban, *ACS Appl. Mater. Interfaces* **2020**, *12*, 16922-16929.
[3] Z. Alsudairy, N. Brown, A. Campbell, A. Ambus, B. Brown, K. Smith-Petty, X. Li, *Mater. Chem. Front.* **2023**, *7*, 3298-3331.
[4] G. Zhang, X. Li, Q. Liao, Y. Liu, K. Xi, W. Huang, X. Jia, *Nat. Commun.* **2018**, *9*, 2785.
[5] X. Li, H. Wang, H. Chen, Q. Zheng, Q. Zhang, H. Mao, Y. Liu, S. Cai, B. Sun, C. Dun, *Chem* **2020**, *6*, 933-944.
[6] L. Guo, L. Yang, M. Li, L. Kuang, Y. Song, L. Wang, *Coord. Chem. Rev.* **2021**, *440*, 213957.
[7] Z. Alsudairy, Q. Zheng, N. Brown, R. Behera, C. Yang, M. Hanif Uddin, A. Saintlima, L. Middlebrooks, J. Li, C. Ingram, X. Li, *Chem. Eng. J.* **2024**, *485*, 149135.
[8] H. Xu, S. Tao, D. Jiang, *Nat. Mater.* **2016**, *15*, 722.
[9] S. J. Lyle, P. J. Waller, O. M. Yaghi, *Trends Chem.* **2019**, *1*, 172-184.
[10] C. Ji, C. Kang, B. C. Patra, D. Zhao, *CCS Chem.* **2024**, *6*, 856-881.
[11] D. Mullangi, S. Nandi, S. Shalini, S. Sreedhala, C. P. Vinod, R. Vaidhyanathan, *Scientific Reports* **2015**, *5*, 10876.
[12] Y. Li, W. Chen, W. Hao, Y. Li, L. Chen, *ACS Appl. Nano Mater.* **2018**, *1*, 4756-4761.
[13] Y. Li, Y. Han, M. Chen, Y. Feng, B. Zhang, *RSC Adv.* **2019**, *9*, 30937-30942.
[14] X. Li, C. Yang, B. Sun, S. Cai, Z. Chen, Y. Lv, J. Zhang, Y. Liu, *J. Mater. Chem. A.* **2020**, *8*, 16045-16060.

[15] J. Hu, Z. Huang, Y. Liu, *Angew. Chem. Int. Ed.* **2023**, *62*, e202306999.
[16] a) H. Chen, D. Feng, F. Wei, F. Guo, A. K. Cheetham, *Angew. Chem. Int. Ed.* **2025**, *64*, e202415454; b) M. Zhang, J. Chen, S. Zhang, X. Zhou, L. He, M. V. Sheridan, M. Yuan, M. Zhang, L. Chen, X. Dai, F. Ma, J. Wang, J. Hu, G. Wu, X. Kong, R. Zhou, T. E. Albrecht-Schmitt, Z. Chai, S. Wang, *J. Am. Chem. Soc.* **2020**, *142*, 9169-9174; c) A. M. Elewa, I. M. Mekhemer, A. F. EL-Mahdy, A. Sabbah, S. Y. Chen, L. Y. Ting, S. Abdelnaser, H. H. Chou, *Small* **2024**, 2311472; d) C. Harrod, Z. Alsudairy, Q. Zheng, A. Campbell, N. Brown, M. H. Uddin, S. Cai, X. Li, *Adv. Sustain. Syst.* **2025**, *9*, 2400700.
[17] a) M. Matsumoto, R. R. Dasari, W. Ji, C. H. Feriante, T. C. Parker, S. R. Marder, W. R. Dichtel, *J. Am. Chem. Soc.* **2017**, *139*, 4999-5002; b) D. Zhu, Z. Zhang, L. B. Alemany, Y. Li, N. Nnorom, M. Barnes, S. Khalil, M. M. Rahman, P. M. Ajayan, R. Verduzco, *Chem. Mater.* **2021**, *33*, 3394-3400; c) X. Shi, L. Yi, H. Deng, *Science China Chemistry* **2022**, *65*, 1315-1320.
[18] a) A. Laemont, G. Matthys, R. Lavendomme, P. Van Der Voort, **2024**; b) X. Kong, Z. Wu, M. Strømme, C. Xu, *J. Am. Chem. Soc.* **2023**, *146*, 742-751.
[19] J.-L. Do, T. Friščić, *ACS Cent. Sci.* **2017**, *3*, 13-19.
[20] a) T. Friščić, C. Mottillo, H. M. Titi, *Angew. Chem. Int. Ed.* **2020**, *132*, 1030-1041; b) A. Krusenbaum, S. Grätz, G. T. Tigineh, L. Borchardt, J. G. Kim, *Chem. Soc. Rev.* **2022**, *51*, 2873-2905; c) S. Głowniak, B. Szczęśniak, J. Choma, M. Jaroniec, *Materials Today* **2021**, *46*, 109-124.
[21] B. P. Biswal, S. Chandra, S. Kandambeth, B. Lukose, T. Heine, R. Banerjee, *J. Am. Chem. Soc.* **2013**, *135*, 5328-5331.
[22] a) G. Das, D. B. Shinde, S. Kandambeth, B. P. Biswal, R. Banerjee, *Chem. Commun.* **2014**, *50*, 12615-12618; b) S. Karak, S. Kandambeth, B. P. Biswal, H. S. Sasmal, S. Kumar, P. Pachfule, R. Banerjee, *J. Am. Chem. Soc.* **2017**, *139*, 1856-1862.
[23] a) N. Brown, Z. Alsudairy, R. Behera, F. Akram, K. Chen, K. Smith-Petty, B. Motley, S. Williams, W. Huang, C. Ingram, X. Li, *Green Chem.* **2023**, *25*, 6287-6296; b) S. T. Emmerling, L. S. Germann, P. A. Julien, I. Moudrakovski, M. Etter, T. Friščić, R. E. Dinnebier, B. V. Lotsch, *Chem* **2021**, *7*, 1639-1652.
[24] S. Hutsch, A. Leonard, S. Graetz, M. V. Höfler, T. Gutmann, L. Borchardt, *Angew. Chem. Int. Ed.* **2024**, e202403649.
[25] E. Hamzehpoor, F. Effaty, T. H. Borchers, R. S. Stein, A. Wahrhaftig-Lewis, X. Ottenwaelder, T. Friščić, D. F. Perepichka, *Angew. Chem. Int. Ed.* **2024**, e202404539.
[26] N. Brown, Q. Zhang, Z. Alsudairy, C. Dun, Y. Nailwal, A. Campbell, C. Harrod, L. Chen, S. Williams, J. J. Urban, Y. Liu, X. Li, *ACS Sustain. Chem. Eng.* **2024**, *12*, 13535-13543.
[27] R. Gao, N. Zhong, L. Tong, X. Kou, W. Huang, H. Yang, S. Huang, J. Wu, G. Chen, G. Ouyang, *Cell Rep. Phys. Sci.* **2022**, *3*.
[28] Y. Guo, X. Liu, X. Liu, N. Xu, X. Wang, *Dalton Trans.* **2023**, *52*, 12264-12270.
[29] X. Zhao, P. Pachfule, S. Li, T. Langenhahn, M. Ye, G. Tian, J. Schmidt, A. Thomas, *Chem. Mater.* **2019**, *31*, 3274-3280.
[30] K. Wang, X. Qiao, H. Ren, Y. Chen, Z. Zhang, *J. Am. Chem. Soc.* **2025**.
[31] J. Hu, S. K. Gupta, J. Ozdemir, H. Beyzavi, *ACS Appl. Nano Mater.* **2020**, *3*, 6239-6269.
[32] M. Zhang, Y. Li, W. Yuan, X. Guo, C. Bai, Y. Zou, H. Long, Y. Qi, S. Li, G. Tao, C. Xia, L. Ma, *Angew. Chem. Int. Ed.* **2021**, *60*, 12396-12405.
[33] L. Xu, S.-Y. Ding, J. Liu, J. Sun, W. Wang, Q.-Y. Zheng, *Chem. Commun.* **2016**, *52*, 4706-4709.
[34] Y. Kumar, I. Ahmad, A. Rawat, R. K. Pandey, P. Mohanty, R. Pandey, *ACS Appl. Mater. Interfaces* **2024**, *16*, 11605-11616.
[35] Z. Zheng, Q. Lin, Y. Gao, X. Ji, J. L. Sessler, H. Wang, *Coord. Chem. Rev.* **2024**, *511*, 215860.
[36] a) X. Guan, Z. Shen, L. Chen, C. Zhang, C. Sun, Y. Du, B. Hu, C. Gao, *ACS Appl. Nano Mater.* **2024**, *7*, 27318-27324; b) Z. Wang, Y. Huang, *New Journal of Chemistry* **2023**, *47*, 3668-3671; c) H. Li, D. Zhang, K. Cheng, Z. Li, P.-Z. Li, *ACS Appl. Nano Mater.* **2023**, *6*, 1295-1302; d) S. An, X. Zhu, Y. He, L. Yang, H. Wang, S. Jin, J. Hu, H. Liu, *Ind. Eng. Chem. Res.* **2019**, *58*, 10495-10502.